

PASSIVE DETECTION OF OBJECTS NEAR A FOUR-ELEMENT PATCH ARRAY

by
Ian Smith

Senior Thesis in Electrical Engineering
University of Illinois at Urbana-Champaign
Advisor: Dr. Jennifer Bernhard

May 2019

Abstract

This thesis has two parts. The first and foremost part was to design a patch antenna array of four elements that operates at 2.4 GHz. It was necessary that the patch array have adequate performance in return loss, specifically at the resonant frequency, and that the elements were separated enough to detect individual element differences in the return-loss parameter. The second part was designing and simulating a procedure to observe S-parameter changes when electrically conductive objects were placed near the array. Data from simulations was observed and recorded. This thesis outlines a first-order algorithm to passively detect objects near a functional antenna array through monitoring the S-parameters of each element of the array.

Keywords: S-parameter, return loss, object detection, passive, patch antenna, reflection coefficient, coupling

Acknowledgments

I would like to thank Professor Bernhard for being willing to advise this thesis. She provided invaluable guidance and helped me develop intuition in approaching this problem. I would also like to thank her research group for assisting me with this thesis. Specifically, I would like to mention Elias Wilken-Resman, who aided me with the milling machine for the array fabrication. Finally, I would like to thank Pallavi Sharma, who patiently and consistently helped me with almost every aspect throughout this whole process. Without her advice and direction, this thesis would not be half of what it is.

Contents

1. Motivation and Existing Research.....	1
2. Patch Antenna Theory.....	2
3. Design of the Antenna.....	3
4. Detune Simulations.....	11
5. Conclusion and Future Work.....	20
References.....	21

1. Motivation and Existing Research

Communication frequencies keep getting higher and higher to accommodate faster speeds. For example, 4G (LTE) to 5G is an increase of around 26 GHz, when considering the main bands, and can be even higher in the future. The downside of higher frequencies, however, is massive attenuation through objects. It will be necessary to sense nearby and potentially signal-attenuating objects, so that a decision can be made about which repeater the antenna should look for.

Most research concerning object detection is sparse, and the object detection is not truly passive. Almost everything deals with sending some type of signal through a transmission (TX) path and receiving the reflected signal off of the object in question through a receive (RX) path. Sometimes research will circumvent this problem by using an “opportunistic illuminator,” essentially, a transmitted signal that is present that the system did not produce (such as a TV or FM broadcast) [1]. Again, this is not what this thesis is concerned about. Instead of using the signal to infer the presence of an object, the actual detune of the antenna serves that purpose. For this detune to occur, the object needs to be electrically close to the antenna (in most cases). Little previous research has been conducted upon this subject.

A case could be made that monitoring S-parameters is not truly passive either because power is being sent to the antenna. This is a fair point, but for the purposes of this thesis, a passive system is one that need not transmit a dedicated TX signal or receive a dedicated TX signal. Perhaps more accurately, monitoring S-parameters is quasi-passive at best.

2. Patch Antenna Theory

A patch antenna is comprised of two pieces of conductive material, separated by some distance d of some dielectric, with dielectric constant ϵ_r . In most cases, this dielectric has a permeability of free space, and a permittivity of $\epsilon_r\epsilon_0$.

One of the conductors (the patch) is driven against the other (the ground) with some sinusoidal signal. There are different methods for delivering this signal to the patch. The two most pertinent to this thesis will be discussed, although there are others (such as aperture-coupled). The first is edge-feed. This is where a microstrip is connected to the patch, parallel to the frequency-determining dimension. For most edge-feed cases, some transform or inset is employed to minimize reflected power. The second method is coax-feed, where a coaxial cable (usually with a characteristic impedance of $50\ \Omega$) is connected to a chosen spot on the patch. The outer part of the coaxial cable is connected to the ground, and the inner pin goes through the dielectric, and is connected to the patch.

The reflection coefficient, or the S_{xx} Parameter, is a crucially important aspect of an antenna. Its formal definition is stated in (1) and is usually expressed in dB.

$$dB\ value = 10 \cdot \log_{10} \left(\frac{P_{incident}}{P_{reflected}} \right) [dB]$$

(1)

As is clear from (1), it is a ratio of the incident power to the reflected power sent to an antenna. Theoretically, if an antenna (in this case, the first port of the antenna) is perfectly matched to its source, then:

$$S_{11} \rightarrow -\infty [dB]$$

In real life, a perfect match between the antenna impedance and the source impedance is impossible; a good enough match yields a S_{xx} of approximately less than -10 dB. A much better match easily can yield a S_{xx} of at least -25 dB.

3. Design of the Antenna

All the patches designed in this thesis were done so on the material Rogers TMM10, which has a constant of 9.2. This was chosen to limit the size of each patch. Each board was 0.635 mm thick and had a 6 in by 6 in ground plane (which was preserved in simulations and fabrication).

Originally, the antenna system was to be comprised of four different arrays, each with four patches. These four patches on each antenna would have a single feed point, and each of the return losses would be monitored. So, it was necessary to design a four-patch antenna with a match to a $50\ \Omega$ source. This was the single most time-consuming part of this thesis. Patches with feeds are complicated, and modern theory only estimates the dimensions of the patches. Electromagnetic coupling makes the system complicated, and optimal points must be found for all the dimensions. However, due to the nature of electromagnetics, these spots are not linear and cannot be solved for independently. Once the optimal dimension for one aspect of the antenna is found, as soon as something else is changed, everything is altered in a manner that is difficult to predict. Theory can be helpful in directing decision making [2]-[7]. To get the antenna working as expected, however, requires delicate tweaking and tuning.

The antenna was initially designed with a feed network, with a coaxial cable in the center to act as the source. A point had to be found where a good match was made, and the phase of each patch constructively interfered. First, that point was solved for using a lumped port in the electromagnetics solver HFSS, and then later a coaxial cable was substituted to get a more accurate simulation. The match for the lumped port was -30.86 dB. After the coaxial cable was substituted, more tweaking was needed. The design, shown in Figure 1, was finalized. Also below are the return loss for the antenna (Fig. 2), and the far field pattern for the antenna (Fig. 3). Note that the quality of the match significantly dropped (from approx. -30 dB to -14 dB). However, the far field pattern is still good, with directivity of around 10 dB. The original idea was to use four of these patch antennas, positioned as shown in Figure 4.

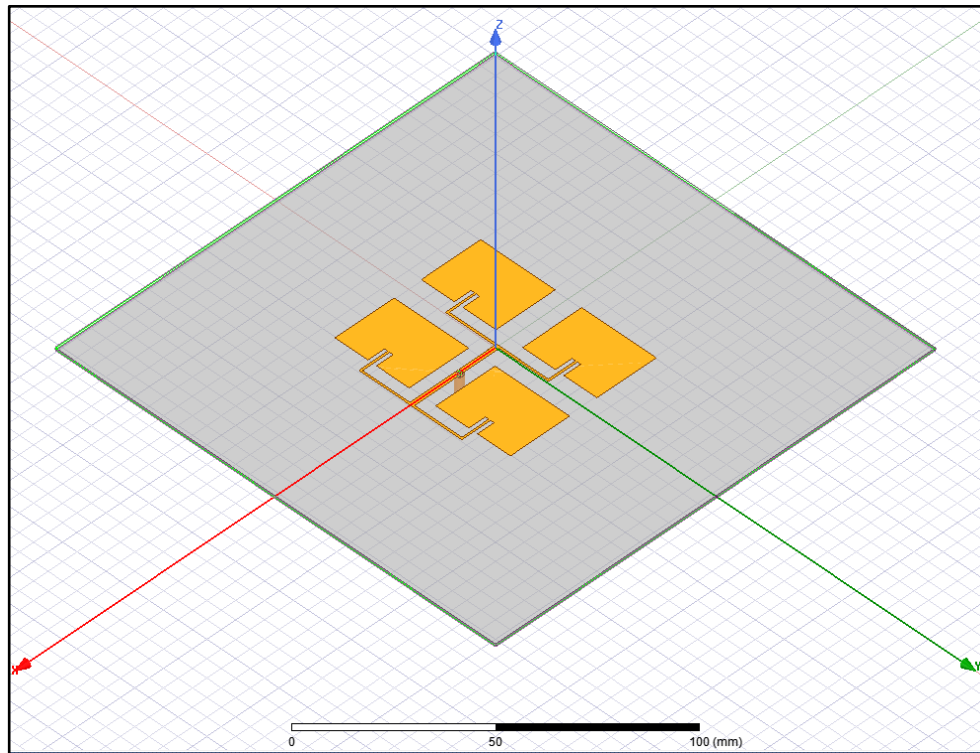


Figure 1. The initial array design.

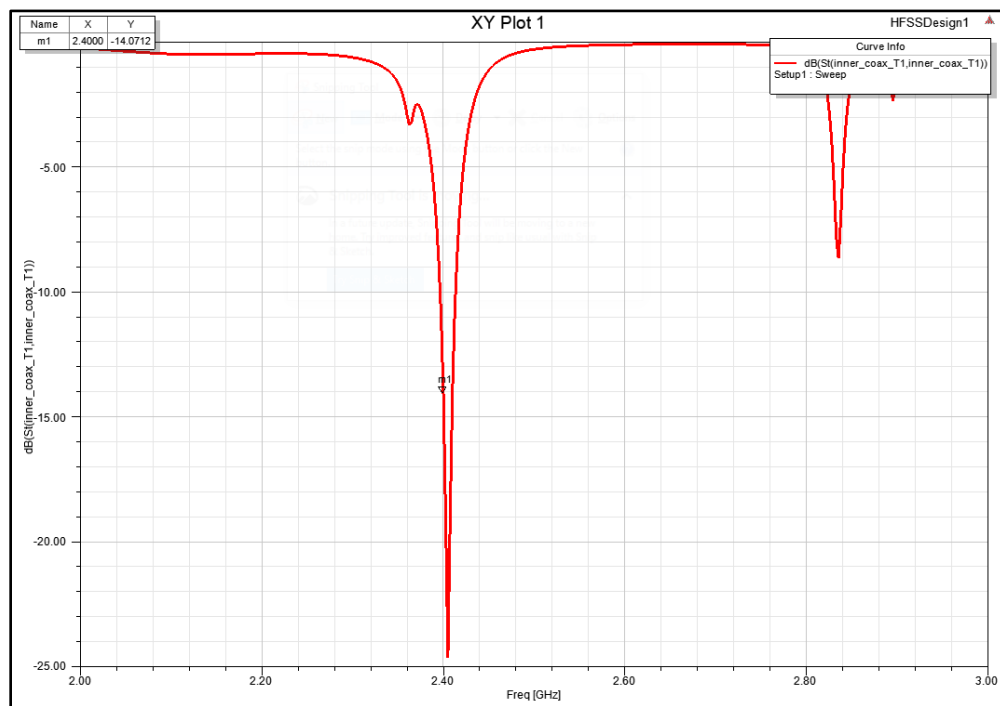


Figure 2. The reflection coefficient plotted across frequency for the first design.

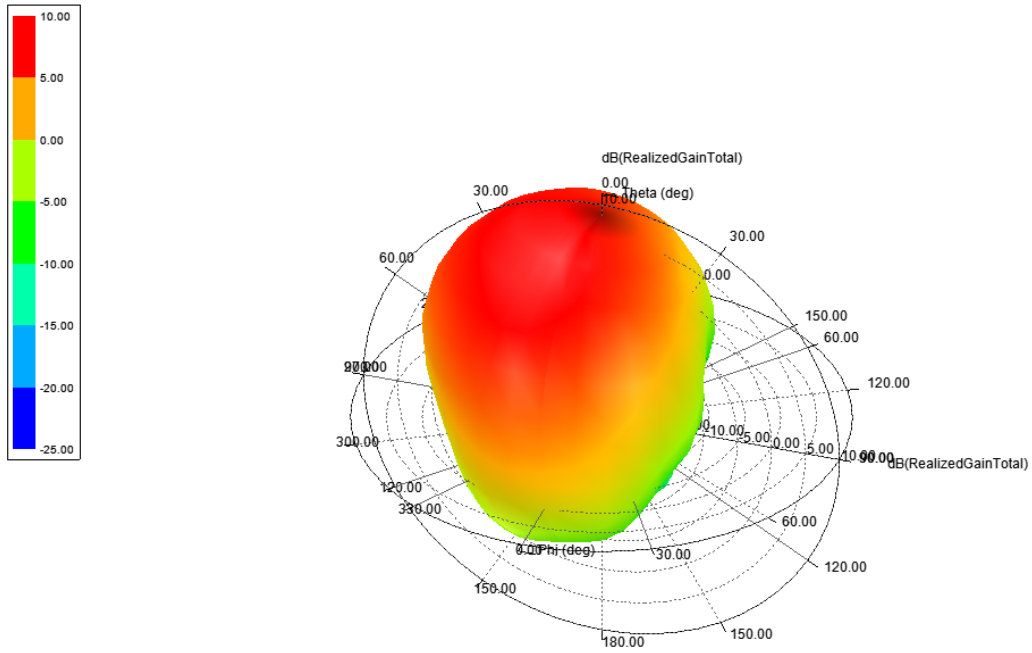


Figure 3. Polar plot of realized gain for the first design.

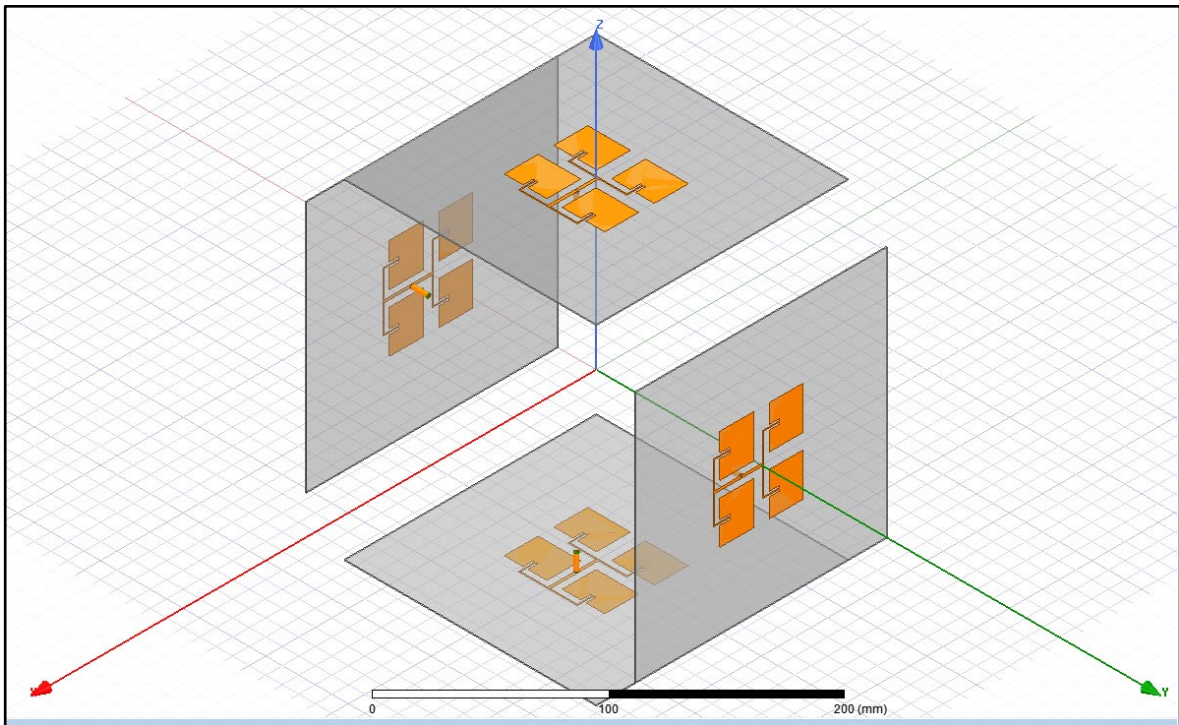


Figure 4. Orientation of four arrays.

With this setup, theoretically, each S-parameter could be monitored, and some information could be gleaned about objects in the near field.

By this point, due to coupling and complication of the design, each simulation required about 26 hours to run. In general, it is necessary to run many simulations to tune the antenna to get a good match. Because of this, it was decided, in the interest of the overall success of the thesis, to simplify the design of the antenna. However, the process of designing this first antenna provided much insight and intuition on how to design patch antennas. Due to this, the design of the second antenna went much quicker.

The second antenna had to be simpler so that many simulations could be run to get an adequate match. Ultimately, it was determined that four individually-fed patches, all in reference to the same ground plane, would suffice. It is necessary that each of the four patches are independently fed so that each of the S_{11} parameters could be monitored for each patch.

As with the first antenna, this antenna was first simulated with idealized lumped ports as excitations, and then with coaxial sources and re-tuned for 2.4 GHz. Figure 5 shows the final design of the coaxial-fed version of the array. Each element of the array had a resonating length of 20.2 mm, and a width of 24.5 mm. Each patch was separated by 90mm in both dimensions, and the coaxial feed point was 3.5 mm offset from the center of each patch.

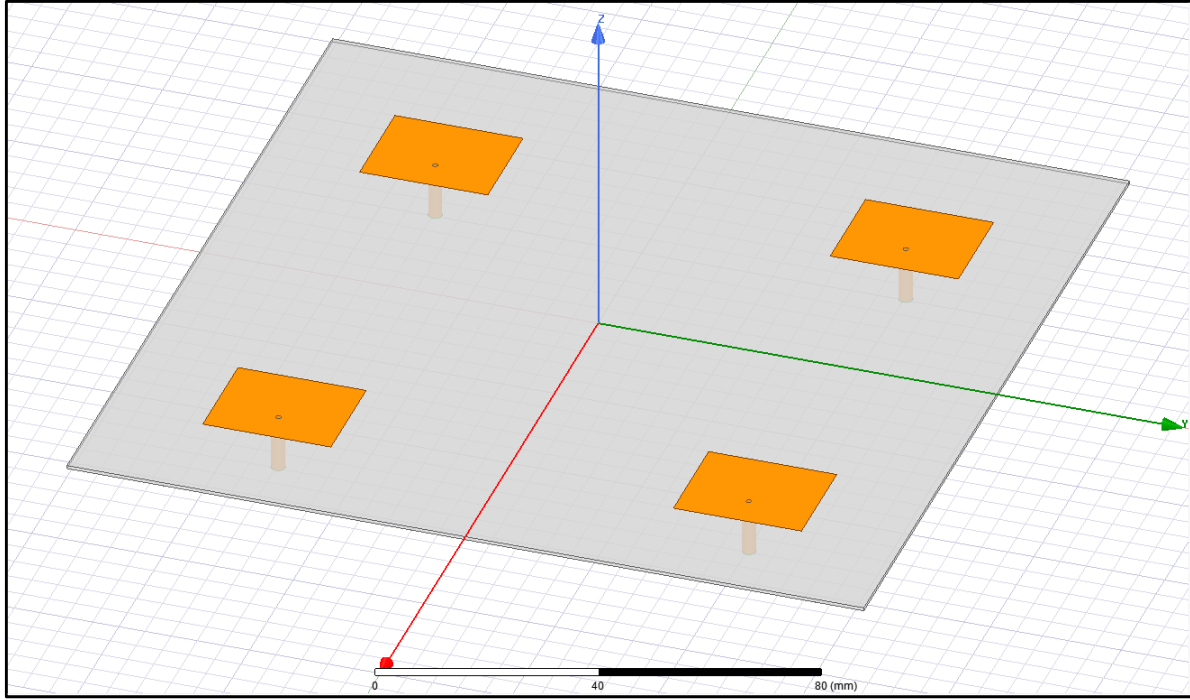


Figure 5. The second and final array design.

As can be seen, these patches are independently fed by $50\ \Omega$ coaxial cables. The S_{11} , S_{22} , S_{33} , and S_{44} coefficients can be seen in Table 1, where the match is measured at a frequency of 2.4 GHz. Figure 6 shows the reflection coefficient plotted across frequency for all ports.

S-Parameter Port	Match [dB]
S_{11}	-11.1360
S_{22}	-10.4236
S_{33}	-10.4214
S_{44}	-10.0465

Table 1. Reflection coefficients for the second design of the array.

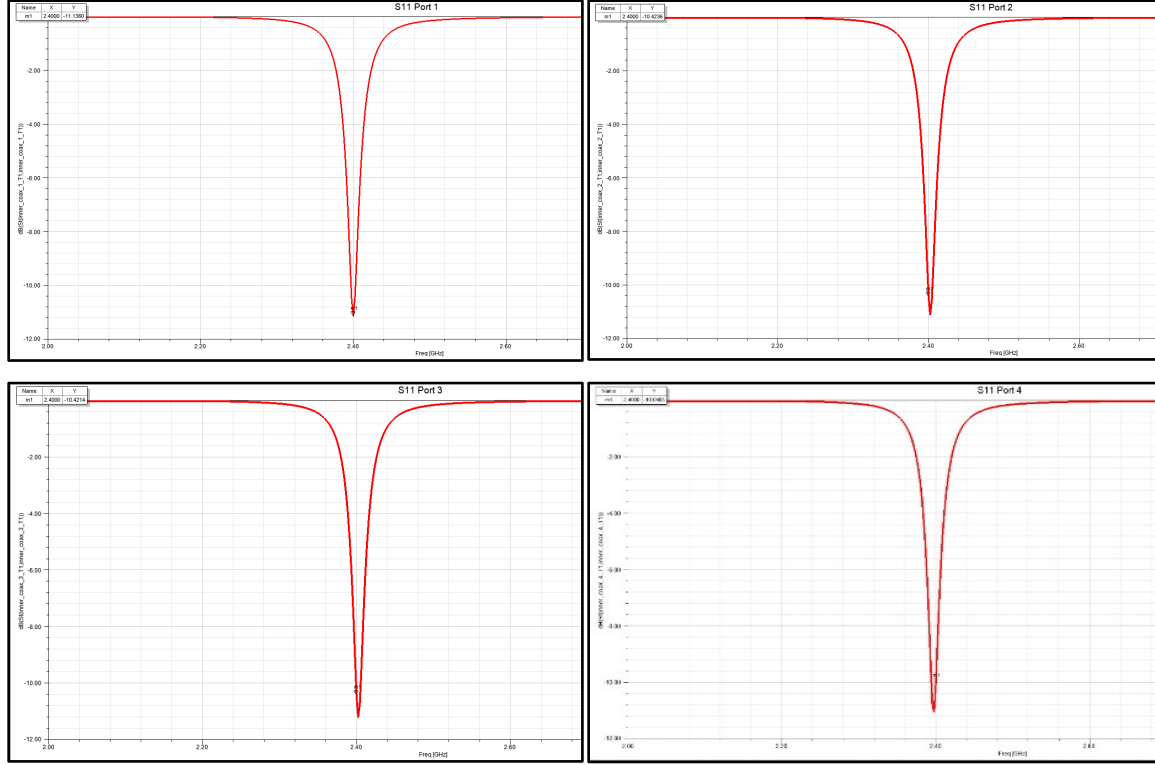


Figure 6. Clockwise from top left: S_{11} plot, S_{22} plot, S_{44} plot, and S_{33} plot.

The matches are good enough for adequate antenna performance, but a decision was made not to make the matches too deep, like on the previous antenna. The reason for this was to sacrifice match quality for match consistency across ports. Once good matches are obtained (say in excess of -25 dB), very minute changes, inconsistencies in manufacturing, and even coupling effects can make the minimum reflection coefficient frequency shift slightly. If the match were too deep, a small shift in resonant frequency might mean the difference between a -25 dB match and a -15 dB match. Since this thesis is about studying the changes in S-parameters due to the presence of nearby objects, the values of each match being consistent takes priority.

Because of these poorer matches, the total realized gain was not as large as before, but was still enough, and maintained a good shape (Fig. 7).

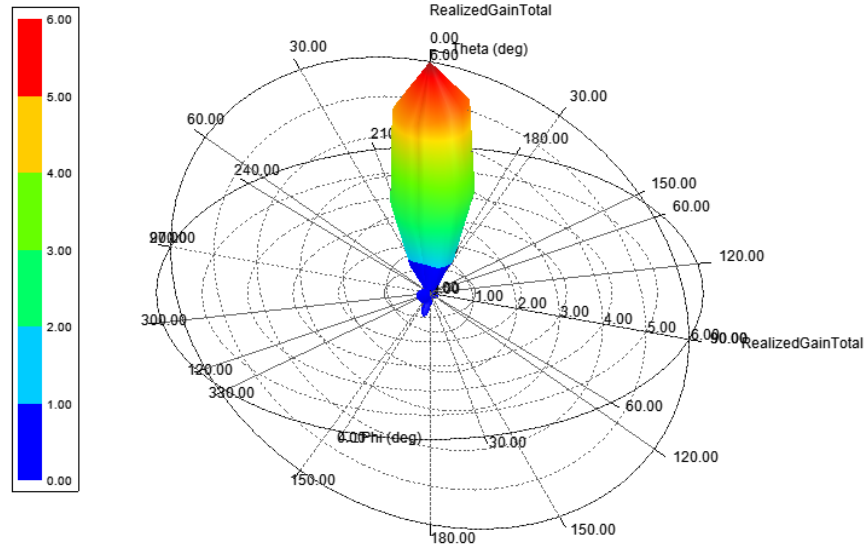


Figure 7. Realized gain plot of the second array.

Another important aspect of the antenna to consider was how much each of the patches contributed towards the total patch radiation. Changing the spacing between the individual patches would result in differing amounts of contribution. Sometimes, at a certain spacing, only one or two patches would contribute in a significant manner. It was important to get all the patches to contribute evenly, within reason, so that they all responded when an object was introduced. Figure 8 shows the electromagnetic field intensity within the dielectric of the whole patch. As can be seen, the individual elements radiate in a fairly even manner.

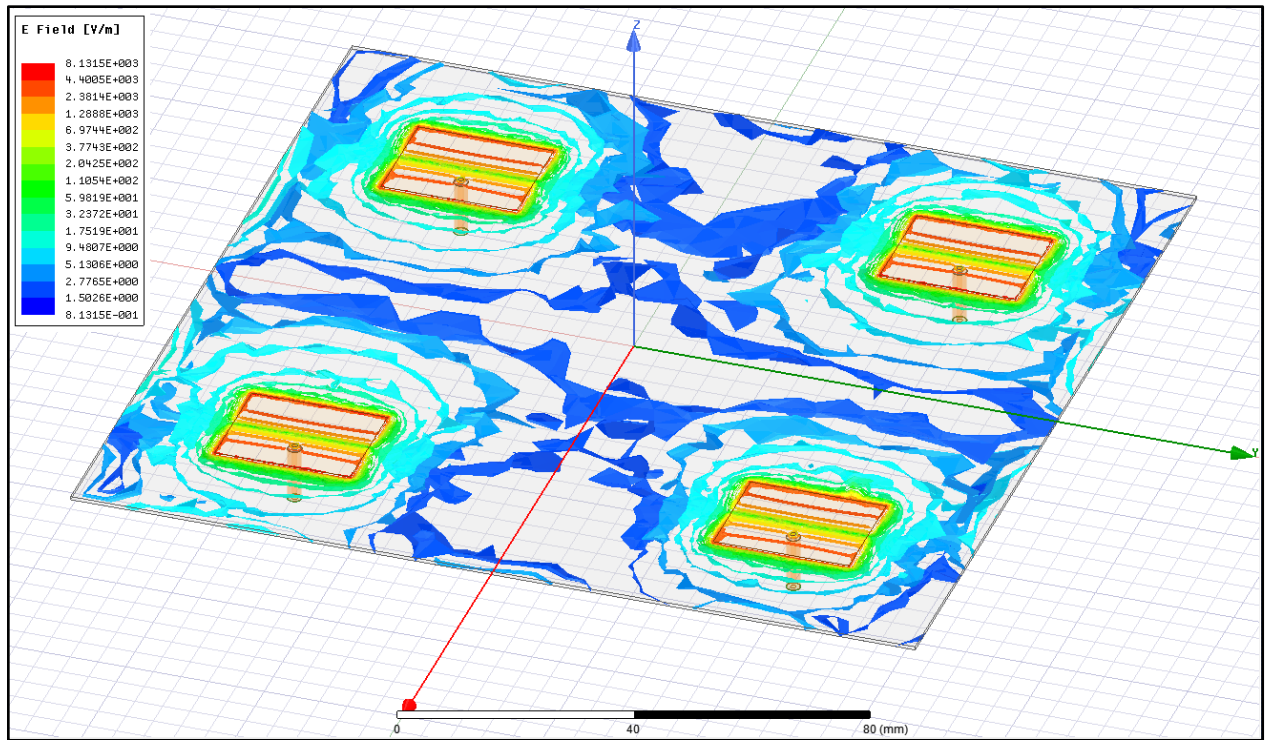


Figure 8. Electric field strength inside the dielectric of the array.

Note: As is usually the case, in Figure 8, blue colors here mean a lower electric field magnitude, while the red indicates the field strength with the highest magnitude. This color scheme does not consider the complete vector of the electric field (which is time dependent), but only the magnitude of said vector.

4. Detune Simulations

In order to assess the viability of detection of objects through monitoring S-parameters, simulations of a nearby object are necessary. An everyday object was chosen (a soda can made from aluminum) and introduced to the near-field of the array. Differing radii ($\frac{1}{16}\lambda$, $\frac{1}{8}\lambda$, $\frac{1}{4}\lambda$, and $\frac{1}{2}\lambda$) and θ (0° , 45° , 90° , 135° , 180° , 225° , 270° , and 315°) around the normal axis of the array were chosen and simulated, and all the S-parameters were recorded. Figure 9, below, shows the different positions that were chosen with respect to the array.

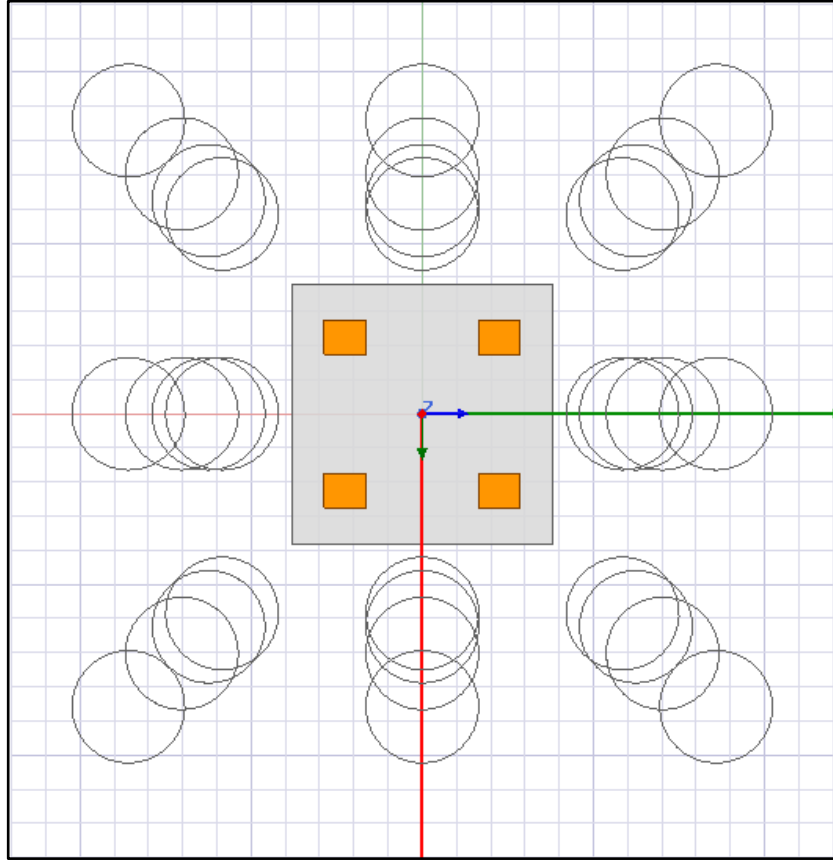


Figure 9. Placement of object for detune simulations.

There are two possible results: one is that there is a predictable change in the S-parameters with changes in the spatial positioning of the object in relation to the array. This is the more desirable outcome because some form of triangulation can be done. This is the lesser likely possibility of the two, because the near field of an antenna is highly non-linear. The other possibility is that

there is very little or no predictability with the changes in the S-parameters. At that point, it is difficult to do triangulation of any kind, so the best option would be to create a Look-Up Table (LUT) and have some error vector established where different positions can be compared in terms of error. Then, the position in the LUT with the least amount of error is selected as the most probable position of the object with respect to the array.

Unfortunately, after the results from the simulations were obtained, very little linearity can be seen. Therefore, the best way forward would be to construct some kind of LUT and error vector. Figures 10 through 19 are the graphs for each S-parameter across θ (each series represents a differing distance).

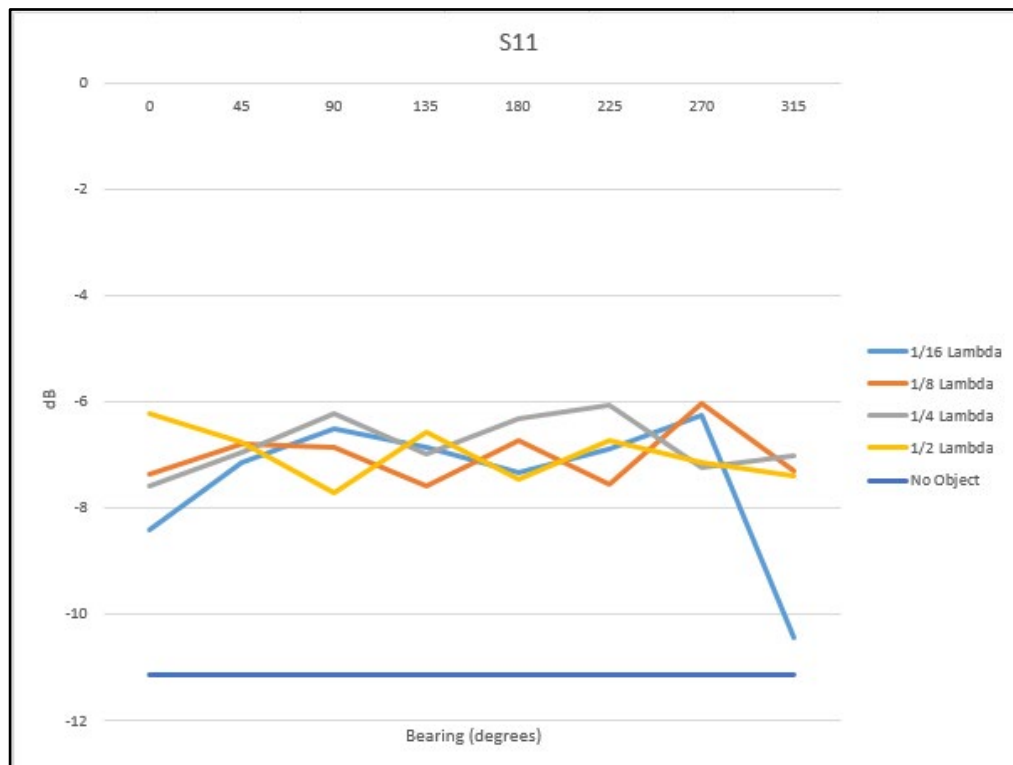


Figure 10. Recorded changes in S_{11} .

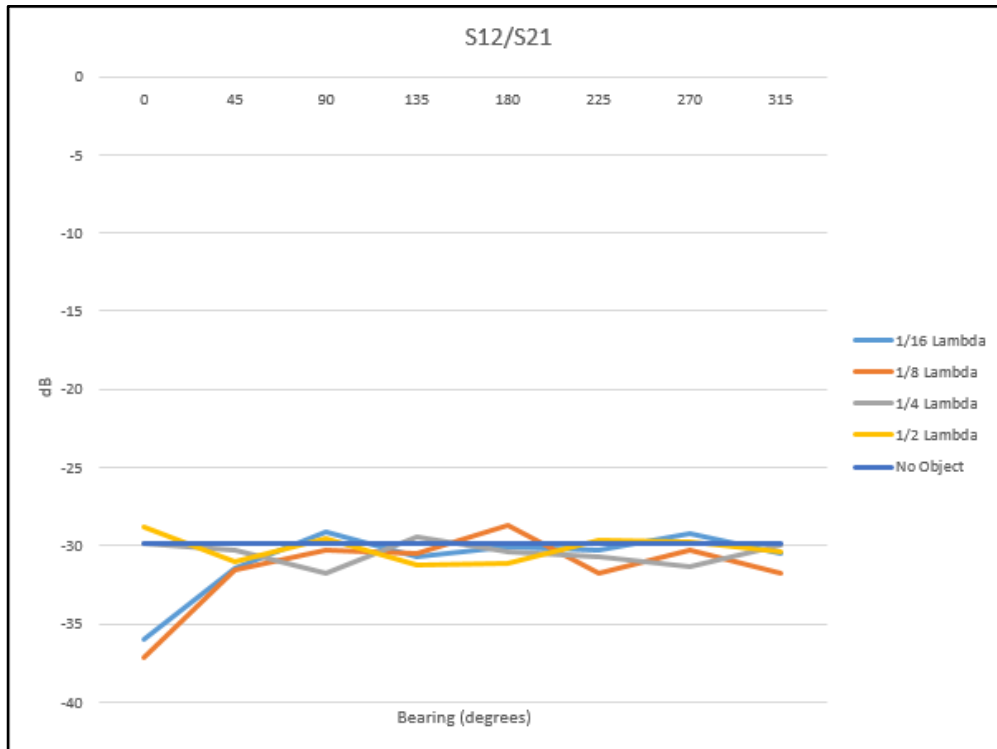


Figure 11. Recorded changes in S_{12} .

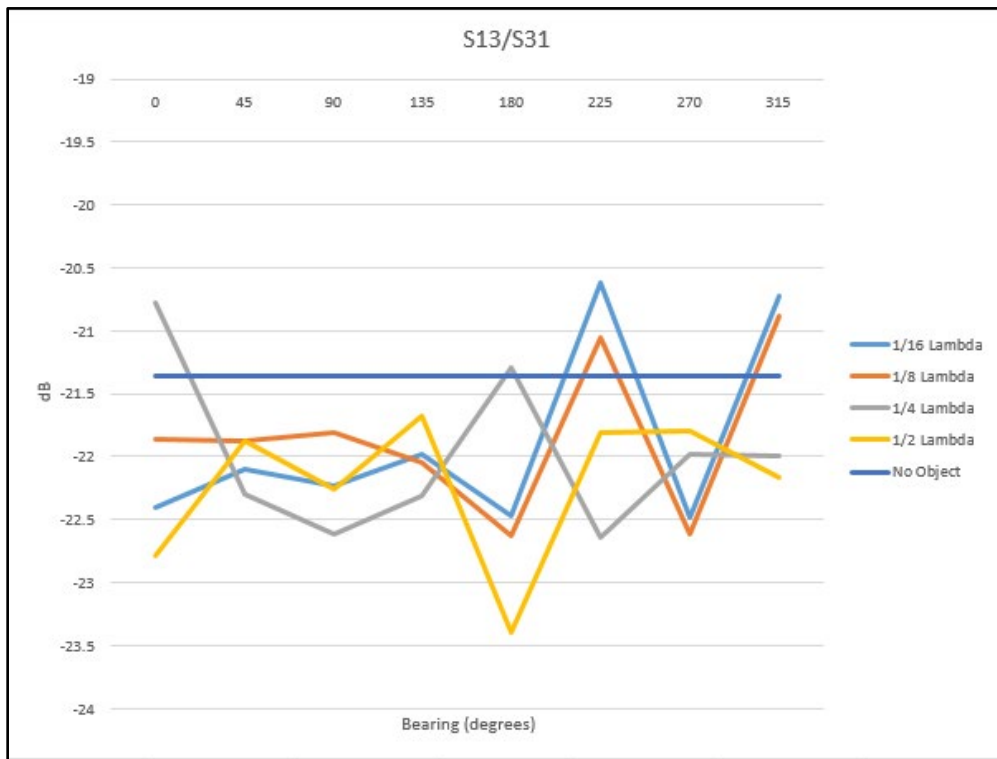


Figure 12. Recorded changes in S_{13} .

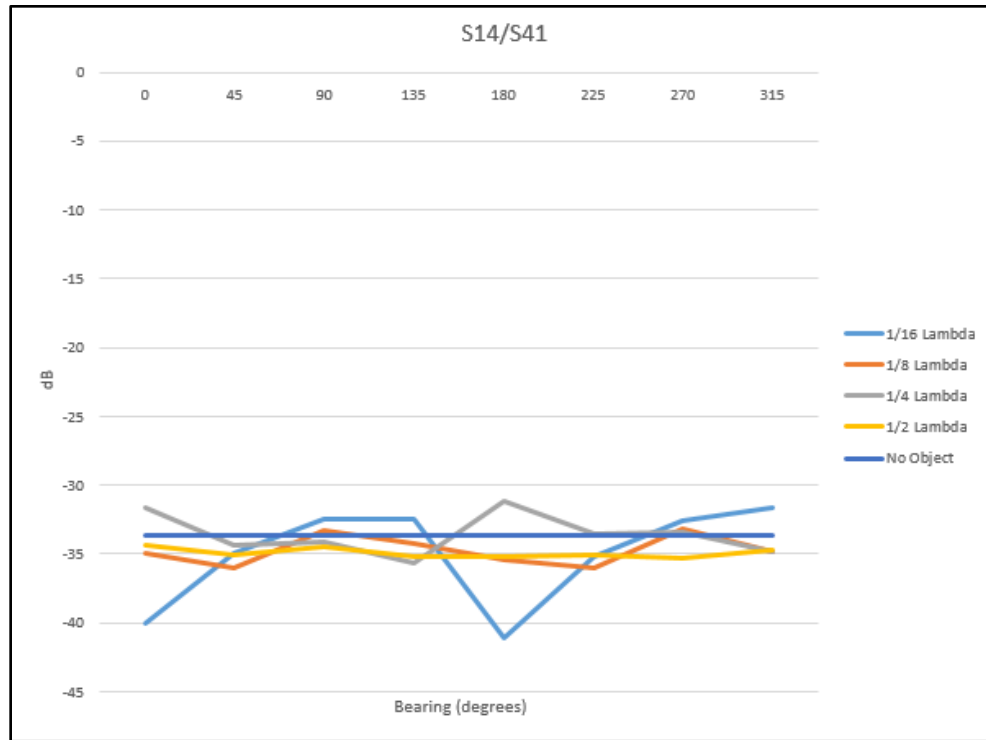


Figure 13. Recorded changes in S_{14} .

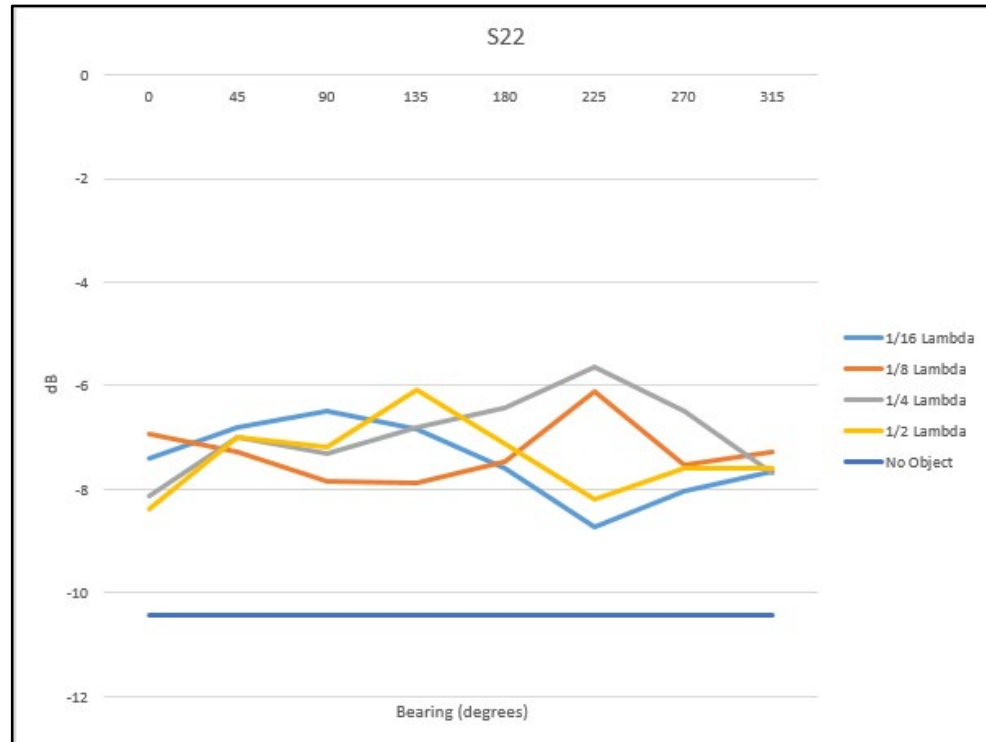


Figure 14. Recorded changes in S_{22} .

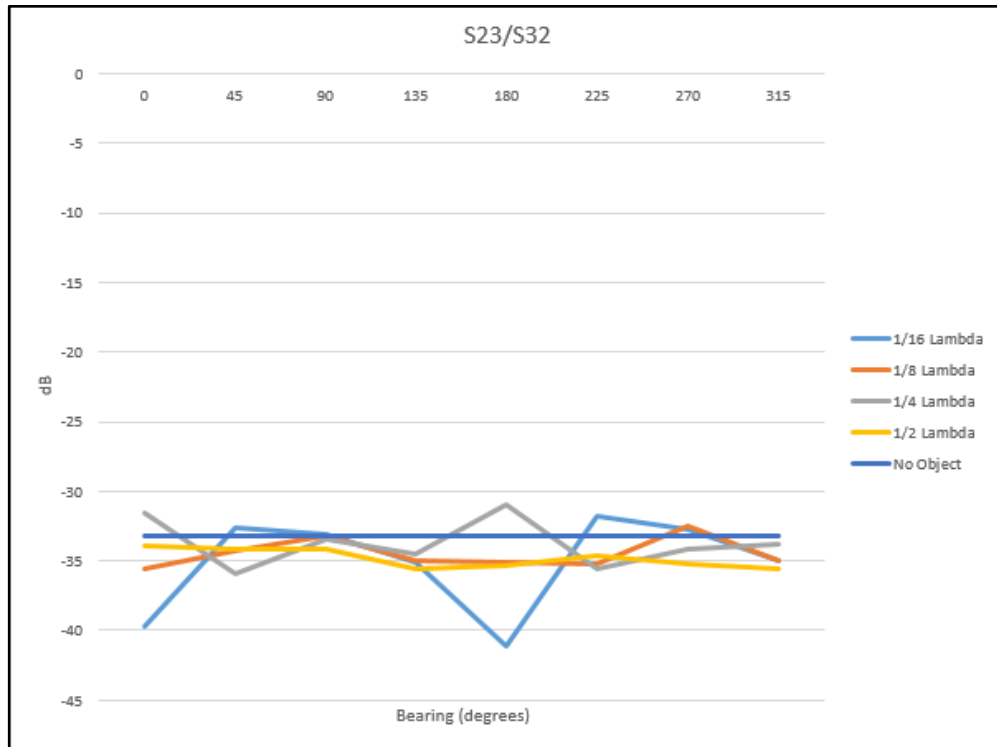


Figure 15. Recorded changes in S_{23} .

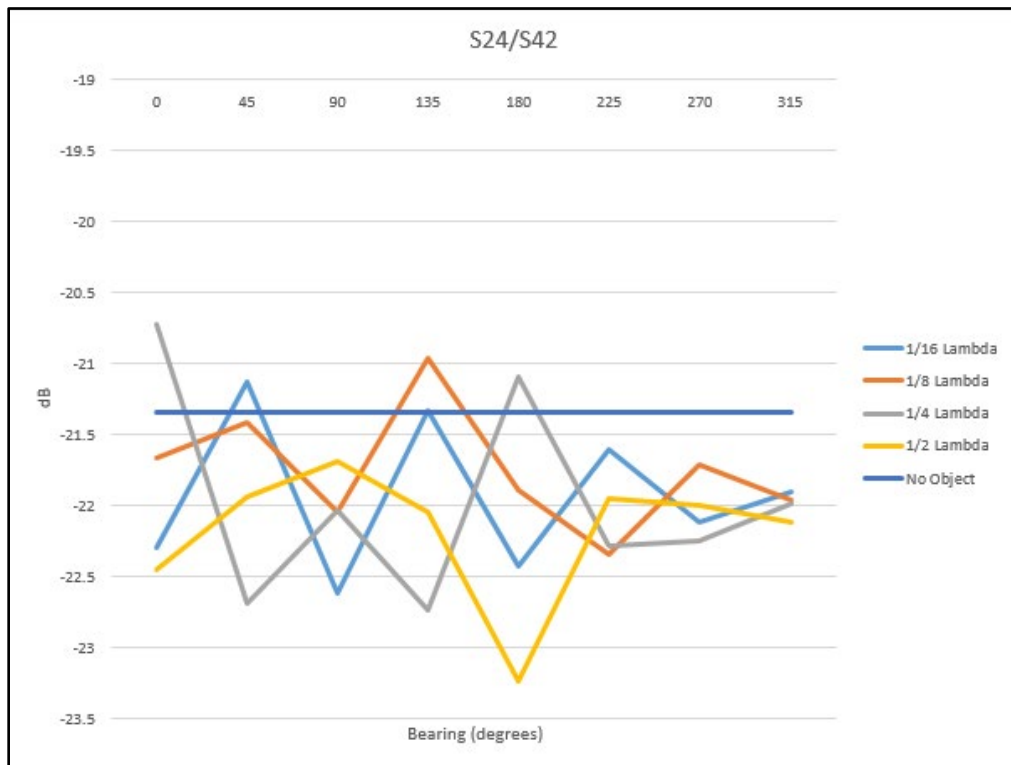


Figure 16. Recorded changes in S_{24} .

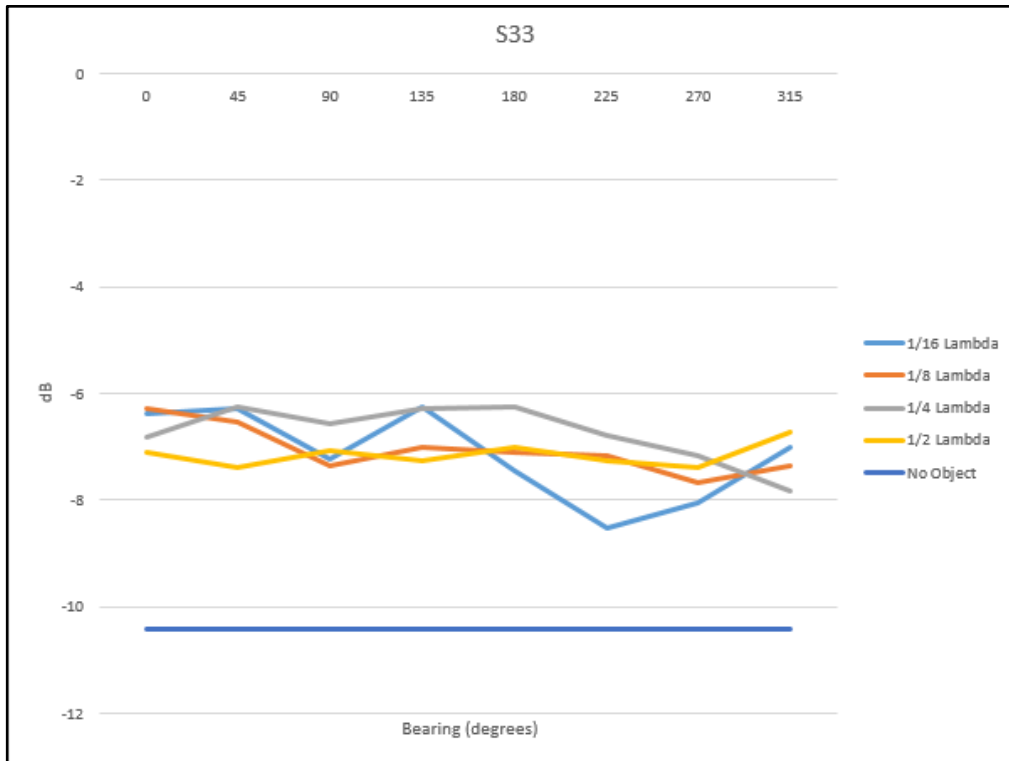


Figure 17. Recorded changes in S_{33} .

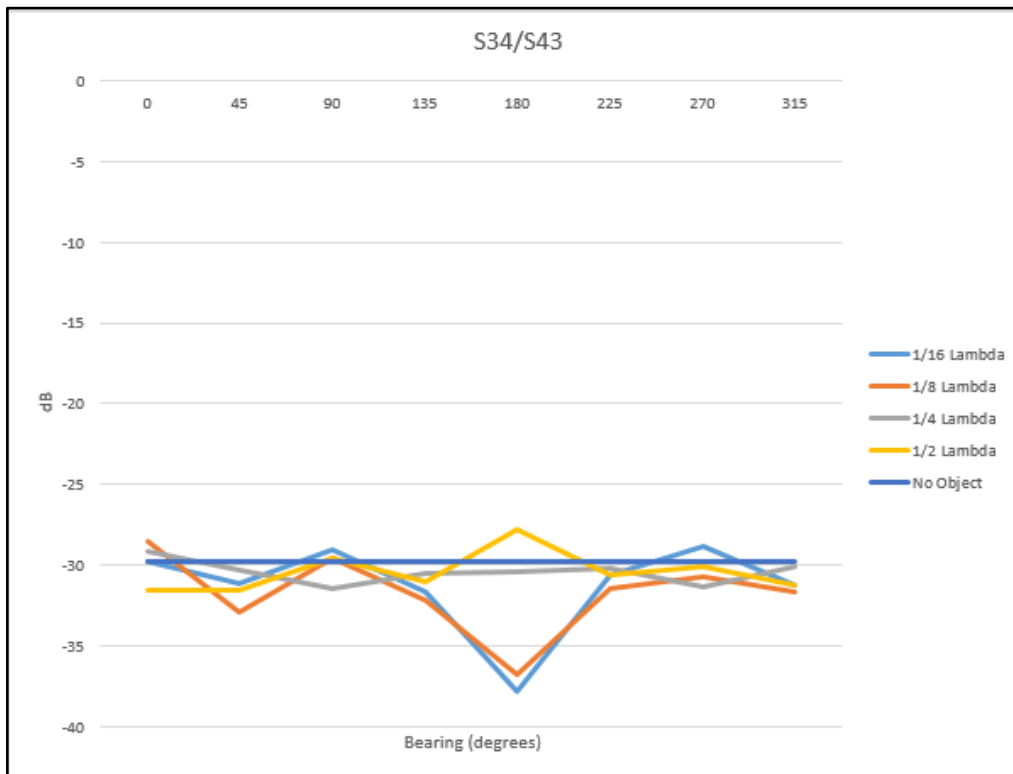


Figure 18. Recorded changes in S_{34} .

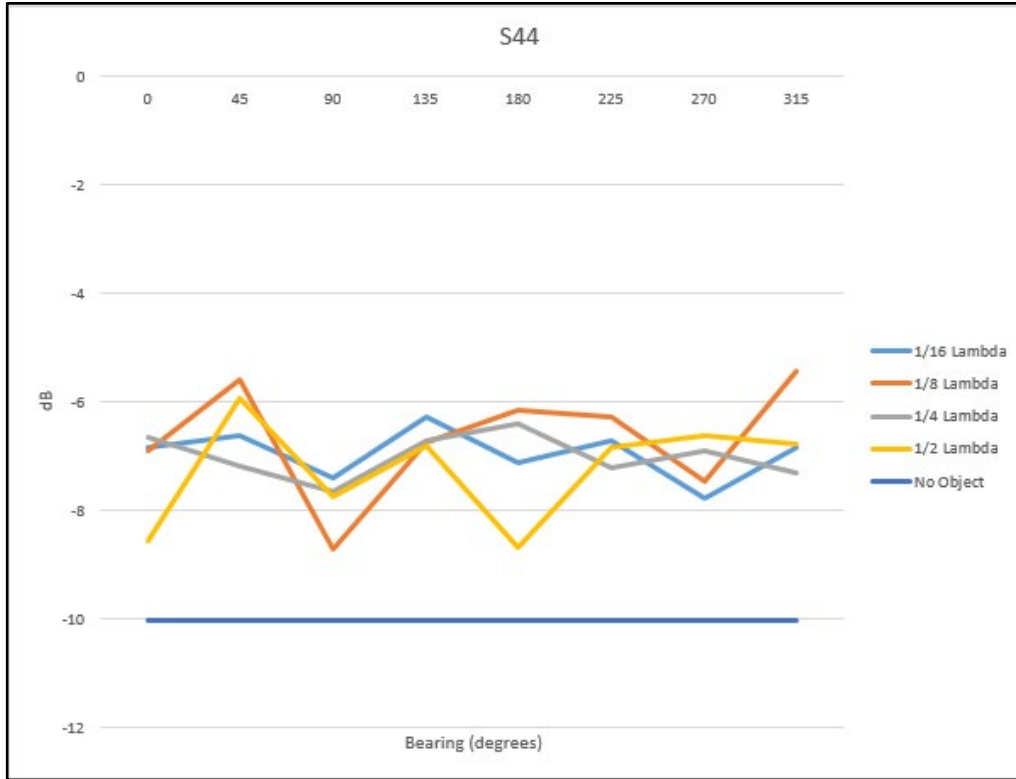


Figure 19. Recorded changes in S44.

Although clear-cut relations are hard to see between S-parameters, distance, and θ ; certain patterns can indeed be distinguished. The clearest and most consistent changes can be seen in the return losses (S_{11} , S_{22} , S_{33} , and S_{44}). These changes always decrease the match, effectively raising the dB at 2.4 GHz. The graphs showing the relationship between the weakly coupled patches (S_{12}/S_{21} , S_{14}/S_{41} , S_{23}/S_{32} , and S_{34}/S_{43}) are basically static and do not change much from the initial conditions, so monitoring them is a waste of resources. The graphs of the strongly coupled patches (S_{13}/S_{31} and S_{24}/S_{42}) show changes in the coupling due to the object. When the object is close to the pair of patches, the coupling variability greatly increases (for S_{13}/S_{31} , this corresponds to a θ range of 225° to 315° , and for S_{24}/S_{42} , this corresponds to a θ range of 45° to 135°). When the object is further away from the pair of coupled patches, the results become a bit less volatile, but there is still a significant decoupling effect. In general, save a few peaks, the presence of the object serves to decouple strongly coupled patches. This makes sense, because the object is a conductor. It is disappointing and slightly surprising that distance did not play a more vital role in the S-parameters. Perhaps the chosen range was too small, and if it had been expanded, a pattern would have been seen. Another possibility is that the dielectric constant of

9.2 is too high to see a significant difference with changes in distance to the patch. With a higher dielectric, the electric fields are more contained, so there is less opportunity for the fields to interact with nearby objects.

As it stands, it would be extremely difficult to interpret where an object is in relation to the array with any level of accuracy from just observing the raw data. Triangulation depends on some form of consistency in the data, so triangulation with S-parameters is not a viable option. To predict where the object is relative to the patch, it might be necessary to train a machine to find patterns in the data. At this point, it becomes a machine learning problem, which is outside the scope of this thesis.

However, a general algorithm for direction finding can be easily obtained. It would look something like that shown in Figure 20.

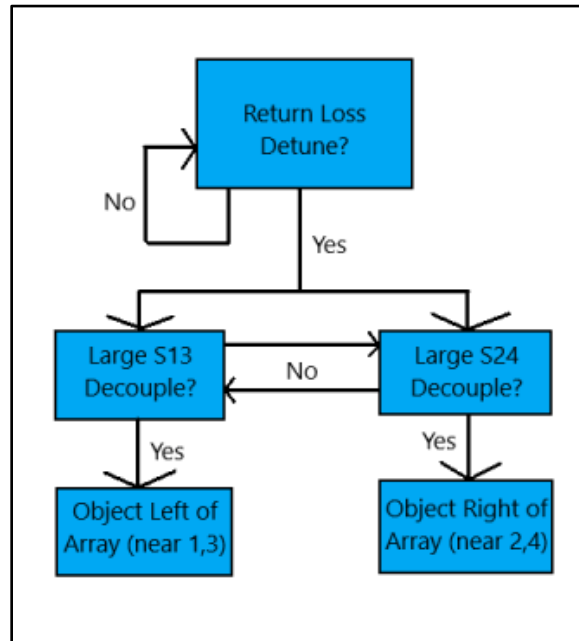


Figure 20. Rudimentary first-order algorithm for determining the position of an object near the array.

If there is an observable shift in return loss from any of the individual patches, then an object is likely in the near field of the antenna. If a high detune is then observed in either pair of strongly

coupled patches, then the object is likely on that side of the array. Of course, this algorithm is extremely general and subject to error. For example, if no large detune is detected in either of the strongly coupled pairs, then this breaks down. Also, as seen from the data, just because an object is near a strongly coupled pair does not mean it must detune that pair to a large degree. The average value of detune approximately maintained the same value at all differing positions of the object, but when the object was nearest the strongly coupled pairs, the peak change increased substantially. It is feasible that even if an object were near a strongly coupled pair, it would not detune the pair excessively; but there is a greater probability it will. In the case where it does not detune excessively, then this algorithm also fails.

5. Conclusion and Future Work

Detecting the nearby presence of an object is certainly possible through monitoring the S-parameters of a four-element patch array. The S-parameters to observe are each return loss, and the S_{xy} , where x and y are strongly coupled patches (in this case 1 and 3, and 2 and 4). The coupling parameters for weakly coupled patches offer almost no information with or without the presence of an object. The largest changes due to the object appear in each return loss. A smaller but still present change occurs in the strongly coupled parameters. Some information regarding the general direction of the object can be obtained through observing the variability of the parameter. If the S_{xy} parameter is variable, then the object is near the side that has those strongly coupled patches. If not, then it is near the side opposite those strongly coupled patches. Because little to no linearity exists, predicting the precise location of the object becomes non-trivial, although an extremely generalized algorithm for direction finding is proposed. Further development and research of this problem could require machine learning.

Because the dielectric of the patch was so high, electric fields (especially the fringe effects) were compact. This was done to keep the patches a manageable size (the higher the dielectric, the lower the patch size at the chosen frequency). However, it is surmised that this hindered the detuning of the patch because there was less field to interact with the object near the patch. Future work would include recreating the patch with a lower dielectric and testing the detune on that patch. Perhaps the detune would be larger or more sensitive. Some additional future work could include developing a better algorithm for the direction finding or introducing the S-parameter data to machine learning. If the direction finding were to become precise enough, this could even be utilized as a passive radar for extremely short-range applications.

References / Bibliography

- [1] X. Zhang, H. Li, J. Liu, and B. Himed, "Joint Delay and Doppler Estimation for Passive Sensing with Direct-Path Interference," *IEEE Transactions on Signal Processing*, 2015.
- [2] C. Balanis, *Antenna Theory - Analysis and Design*. John Wiley & Sons, 2005.
- [3] D. Orban and G. J. K. Moernaut, "The Basics of Patch Antennas, Updated," [Online]. Available: <http://orbanmicrowave.com/wp-content/uploads/2014/12/Orban-Patch-Antennas-2009-rev.pdf>.
- [4] EEWeb. (2019). [Online]. Available at: <https://www.eeweb.com/tools/microstrip-impedance> [Accessed 14 Feb. 2019].
- [5] *Microstrip Patch Antenna Calculator*. [Online]. Available: <https://www.pasternack.com/t-calculator-microstrip-ant.aspx>. [Accessed: 02-Apr-2019].
- [6] K. Murugan, *Design of 2.4 GHz patch antenna for WLAN application*. Proceedings of the IEEE, 2015.
- [7] Y. Hu, D. R. Jackson, J. T. Williams, S. A. Long, and V. R. Komanduri, "Characterization of the Input Impedance of the Inset-Fed Rectangular Microstrip Antenna," *IEEE Transactions on Antennas and Propagation*, vol. 56, no. 10, pp. 3314-3318, Oct. 2008.